Exhibit

Extended theory of selective photothermolysis

G.B. Altshuler (PhD)[1], R.R. Anderson (MD)[2], D. Manstein (MD)[2], H.H. Zenzie (MS)[1], and M.Z. Smirnov (PhD)[3]

[1]Palomar Medical Technologies, Inc., Burlington, MA 01803

[2]Massachusetts General Hospital, Wellman Laboratories of Photomedicine, Boston, MA 02114

[3]Institute of Fine Mechanics and Optics, St. Petersburg, Russia 197101

Key words: photothermolysis, photoepilation, photosclerotherapy

Abstract

Background and Objective: We present a new theory of selective thermal damage of non-uniformly pigmented structures in biological tissues. Spatial separation of the heavily pigmented areas and the target requires limitation of the pigment temperature and heat diffusion from the pigmented to the targeted areas.

Study Design/Materials and Methods: A theoretical model of selective target damage by heat diffusion is presented for three target geometries: planar, cylindrical, and spherical. An in vitro experiment is described in which the dependence of thermal damage on pulsewidth at constant fluence was evaluated.

Results: The in vitro experiment showed that the size of the damage zone for similar hair follicles was pulsewidth independent over a very broad range of pulsewidths (30 to 400 ms). We formulated a new theory (extended theory of photothermolysis) to interpret the experimental results.

Conclusions: Based on this new theory, the treatment pulsewidth for non-uniformly pigmented targets is significantly longer than the target thermal relaxation time. The theory provides new recommendations for photoepilation and photosclerotherapy parameters.

Introduction

For many years electromagnetic radiation (EMR) from lasers, lamps and other EMR sources (including microwave ones) have been used to treat a variety of medical conditions in ophthalmology, dermatology, urology, otolaryngology and other specialties. For example in dermatology EMR sources have been used to perform a wide variety of procedures including hair removal, treatment of various pigmented lesions, removal of unwanted veins, tattoo removal, and skin resurfacing. For all these treatments, a natural or artificial chromophore present in the body is heated by

absorption of either monochromatic or broadband EMR. Typical natural chromophores include water, melanin, hemoglobin, protein, lipid, etc.. Artificial chromophores can include dye, ink, carbon particles, etc. For example, heating of a chromophore may result directly in the destruction of a tattoo or a pigmented lesion. In these cases, the treated target for destruction and the chromophore occupy the same area. These cases are very well described by the theory of selective photothermolysis [1]. The theory of selective photothermolysis provides a quantitative description of optical treatments such as those mentioned above. The aim of selective photothermolysis (SP) is to provide permanent thermal damage of targeted structures with the surrounding tissue held intact. To satisfy the above criterion, the EMR pulsewidth τ must be small compared to the thermal relaxation time (TRT) of the whole target. Actually, if the condition $\tau << TRT$ is met, the heat generated within the target due to EMR absorption does not flow out of the structure until it becomes fully damaged (coagulated, injured). The above approach provides both selective damage and minimum light energy deposition.

However, the use of such a short pulsewidth becomes inapplicable when the target absorption is non-uniform over its area and part of the target exhibits weak or no absorption, but the other part exhibits significant absorption. If this is the case, the weakly absorbing part of the target has to be damaged by heat diffusion from the highly pigmented/strongly absorbing one (hereafter called the *heater* or *absorber*). An example of such a target is the hair follicle [2]. The highly absorbing areas consist of melanin-bearing structures, (i.e., the hair shaft and the matrix cells). The other follicular tissues including the stem cells do not contain an appreciable amount of any chromophore that absorbs in the red/near-IR. These targets (tissues) can be damaged by heat diffusion from the hair shaft or the matrix cells to the surrounding follicular structures. Another example is the treatment of telangiectasia or leg veins

with a wavelength near the maximum hemoglobin absorption. Permanent closure of a vascular malformation or a vein probably requires coagulation of the vascular or vein wall [3]. In this case, coagulation of the wall requires heat diffusion from blood to wall.

In this paper we will demonstrate the heat diffusion concept by presenting the results of a simple in vitro experiment involving a hair follicle. Then, we will discuss the mechanism and the requirements for selective damage of biological structures by heat diffusion. We will prove these new concepts using thermal diffusion theory for isolated plane, cylindrical, and spherical targets. We will apply this theory to high-density targets. Finally, as an example, we will apply this new theory to the cases of hair follicle and spider vein treatment. For readers who are interested in the mathematical details, we have included all theoretical derivations in the Appendix.

The goal of the following experiment was to evaluate the effects of pulse duration and irradiance for a constant fluence on different anatomical structures of the hair follicle. The thermal damage after laser exposure was evaluated by histochemical demonstration of lactate dehydrogenase (LDH) activity.

Material and methods

Post-mortem scalp skin of one donor with light skin and dark brown hair was used for the experiments. The sample was procured 8 hours post mortem, frozen and stored at -80°C. The average hair density was 244 ± 26 hairs/cm^2, and the average hair diameter was 68 ± 12 µm. The hair of the post-mortem scalp sample was clipped to a length of approximately 0.5 mm. From this sample, 6-mm punch biopsies were obtained each containing an average of 69 ± 7 hairs. The biopsies were placed into human, hairless, post-mortem back skin of 3x3 cm^2 size and 1.5-cm thickness that was serving as a frame. In order to obtain good fit, an opening was prepared in the back skin using a 5-mm skin punch. The entire sample was placed on a temperature-

controlled plate. A 120-μm thermocouple was located below the biopsy to monitor the temperature of the specimen. The exposure was performed when an equilibrium temperature of 30±1°C was measured.

The exposures were performed with an 800-nm diode laser prototype with 9-mm spot size and a sapphire window maintained at room temperature. The fluence was kept constant at 35 J/cm^2 for all exposures. The pulsewidth was 30, 100, 200, 350, 400 and 500 ms equivalent to an irradiance of 1170, 350,175,100, 90 and 70 W/cm^2. Before and after each exposure, a dermatoscopic image with crossed polarizing filters was taken (Dermaphot, Heine, Germany).

Histochemical technique: The samples were processed in horizontal frozen sections of 15-μm thickness, and a histochemical evaluation of lactate dehydrogenase (LDH) activity was performed as decribed by Balogh et al. [4]. Representative micrographs were taken at a level close to the bulge.

Results

Evaluation of the dermatoscopic images demonstrated a strong dependence of pulsewidth on the alterations of the clipped hair shafts. For 30-ms pulsewidth, the hair shafts were ablated, and a brownish chromophore was released from the ablated hair shafts (browning). For 100-ms pulsewidth, only coarse and adjacent hair shafts demonstrated some alterations such as apparent thickening and darkening. For exposures with pulsewidths of 200 ms and longer, no hair-shaft alterations were observed at the surface after laser exposure.

Micrographs demonstrating LDH activity at the bulge level are shown in Figures 1 a-e. Hair follicles with similar hair shaft diameter were selected. The inner root sheath (IRS) and the hair shaft (HS) do not possess LDH activity at the bulge level and therefore do not stain blue. Thermal damage of the outer root sheath (ORS)

or perifollicular cellular structures can be assessed by a sharply demarcated pale zone with loss of LDH activity. Selective loss of LDH activity of the ORS was observed for all pulsewidths from 30 to 400 ms. Some hair follicles also had a thin perfollicular cuff with loss of LDH activity. No significant variation of damage-zone diameter was observed with increasing pulsewidths for damaged single hair follicles at a fixed fluence of 35 J/cm^2. The extent of the thermal damage for each hair follicle was correlated to the coarseness and pigmentation of the hair shaft. However, for pulsewidths longer than 200 ms, the percentage of damaged hair follicles decreased with increasing pulsewidths. For a pulsewidth of 500 ms corresponding to an irradiance of 70 W/cm^2, no decrease of LDH activity at the bulge level was observed for any structure. For hair follicles that were located within a few hundred microns of each other, inter-follicular tissue damage was observed for all pulsewidths. This interfollicular damage was related to hair shaft diameter, pigmentation, distance and local hair follicle density.

Theory and discussion

As we can see from the experiment discussed above, the damage-zone size for similar hair follicles is pulsewidth independent over a very broad range of pulsewidths (30 to 400 ms). Based on the classical theory of selective photothermolysis [1], this behavior is very typical for pulsewidths significantly shorter than the target TRT. However, in our case, the pulsewidths are close to or longer than the TRT (not shorter!). The TRT of a hair follicle with a diameter of 200-300 μm is 25-55 ms; our 400-ms pulsewidth is approximately a factor of 7 longer than the maximum TRT! The next surprising result is that, even for relatively high-density targets such as scalp hair follicles, the thermal damage is still selective for

pulsewidths where τ>>TRT. This experimental result stimulated us to investigate the thermal damage process of a target (such as a hair follicle) that has a structure with spatial separation between part of the target and the pigmented area. As we show below, a new theory (the extended theory of selective photothermolysis) was required to correctly interpret our experimental results.

1. Method of selective target damage by heat diffusion

Thermal damage of this type of target (with separation between part of the target and the pigmented area) requires deposition of sufficient heat energy into the absorbing area and good heat exchange between this area and the targeted external structures. Heat deposition depends on the absorption coefficient of the absorber and the EMR power density. Heat exchange depends in turn on the distance between the heater and the outermost part of the target and on the heat transmission coefficient between the absorber and the intervening tissue. However, at a sufficiently high temperature both the heater absorption coefficient and the heat transmission coefficient from the heater to the other targeted tissues may become lower due to phase transitions and destructive processes such as bleaching, melting, boiling, and bubble formation. This results in inefficient use of EMR energy for phase transition processes within the absorber and the intervening tissue. To prevent these undesirable effects, the heater peak temperature has to be limited to a prescribed value, T_{1max}, called hereafter the *collapse temperature*. The collapse temperature T_{1max} of most natural chromophores (e.g. melanin, hemoglobin, and water) exceeds 100^0C. Simultaneously, to ensure permanent damage of the whole target, the temperature should exceed a second prescribed value, the *damage temperature* T_2,

throughout the target area. This temperature is lower than the collapse temperature T_{1max}. More precisely, the damage temperature, T_2, is the temperature at which irreversible thermal damage of the target occurs. We suggest that the basic damage mechanism in soft tissue is the denaturation of proteins. As an alternative to the rigorous Arrhenius rate process integral [5], the dynamic denaturation process may be described approximately by using the simpler damage-temperature concept. For human-skin collagen, T_2 is about 65-75^{0}C and for cells T_2 is about 60^{0}C if the exposure duration is several tens of milliseconds [5]. Furthermore, the tissue temperature should not exceed the water boiling point to prevent formation of vapor bubbles that could insulate the absorbing area from the surrounding tissue. Strictly speaking, vapor bubbles can transfer heat from the absorbing area to the target, but this process is unpredictable because vapor bubbles can move in different directions. To meet the temperature limitations described above, the EMR power must be limited, (but sufficient to heat the target up to the damage temperature) and, therefore, the EMR pulse has to be made sufficiently long to deliver enough energy. We define the *thermal damage time (TDT)* of the target to be the time required for irreversible target damage with sparing of the surrounding tissue. For a non-uniformly absorbing target structure, the TDT is the time when the outermost part of the target reaches the target damage temperature T_2 through heat diffusion from the heater. Because the heat-diffusion front becomes blurred when propagating into the tissue, part of the heat energy will leave the target. Therefore, the heated area will be larger than the damaged area. However, we demonstrate below that target damage can still be selective even though the TDT is many times as long as the TRT of the whole target. Apparently, the *optimum EMR pulsewidth,* τ_0, should be shorter than or equal to the TDT. So, in contrast to the standard theory of selective photothermolysis, non-

uniformly pigmented structures have to be treated by long EMR pulses: the pulsewidth must typically be longer than the target TRT. In addition, the EMR power should be limited to prevent reduction of the heater absorption by bleaching, vaporization, etc.

Figure 2 shows the general structure of a *"target"* that is thermally denatured by heat diffusion from a *"heater"*. The heater includes a natural or artificial chromophore (pigment) with a high photon absorption coefficient. The target exhibits weak EMR absorption. The distance between the heater and the target is d. Photons from the EMR source are absorbed by the heater. As discussed in the previous section, the EMR power density has to be adjusted so that during the time of treatment the heater temperature T_1 does not exceed the temperature T_{1max} where the absorption coefficient may begin to drop. The heat propagates from the heater to the target due to either thermal diffusion or two other possible mechanisms. The two other mechanisms are hot ablation products emanating from the heater or steam. In this paper, we concentrate exclusively on the thermal diffusion mechanism. The process of target thermal damage is finished when its temperature reaches T_2, while the temperature of the surrounding tissue remains below its damage temperature. In general, it is not possible to damage the target without damaging the tissue between the target and the heater. For this target type, precise selective damage of the target is impossible. But if the treated target is a layer or a shell of tissue roughly symmetrical with respect to the heater, the target damage can be made precisely selective. This means that the damage zone covers the whole target without extending beyond it. After the end of the EMR pulse, the target temperature at the outermost point goes on growing until it reaches a maximum. The time delay between the end of the EMR pulse, τ, and the moment when the peak temperature is

reached maximum (the latter is the TDT) is denoted by ε and thus τ_0= TDT - ε. Therefore, the EMR pulsewidth is equal to or shorter than the TDT. This delay ε is roughly equal to the propagation time of the heat front from the heater to the target $\varepsilon \cong d^2/k$, where k is the thermal diffusivity of the tissue (k≅ 0.1 mm^2/s); ε is therefore close to the target TRT. As we shall see subsequently, TDT is significantly longer than the TRT in most cases. So, for selective treatment the pulsewidth should be approximately equal to the TDT: $\tau_0 \cong$TDT. The TDT depends in turn on T_1, T_2, and the target size. For a better understanding of this dependence we first look more closely at heat diffusion from the heater to the target. Specifically, we focus on a target comprising a heavily pigmented long cylinder of diameter d_1 and a surrounding treated area of diameter d_2 (Fig. 3). This simple geometry can be used to model thermal damage of hair follicle by hair shaft heating or blood vessel destruction. We consider two heating modes. The first mode utilizes a *"rectangular EMR pulse"* (Fig. 4a) and the second one utilizes a *"rectangular temperature pulse"* (Fig. 4b). In the case of the rectangular EMR pulse, the heater temperature grows during the EMR pulse and reaches T_1 at the end of the pulse (Fig. 4c). In the case of the rectangular temperature pulse, the temperature of the heater is constant during the EMR pulse, which requires a special pulse shape (Fig. 4d). For both heating modes, the heater temperature is below the collapse temperature T_{1max} so the absorption coefficient of the heater does not change.

The sequence of thermal profiles during the heating process is depicted in figure 3. The input parameters for modeling are d_1 = 70 μm, d_2 = 210 μm. The collapse temperature T_1 is 100°C (the boiling point of water). The damage temperature is 70°C, which is the average protein denaturation temperature in the 10-1000 ms pulsewidth range. We assume that the EMR absorption is confined to

the heater and that the thermal properties of the heater, the target and the surrounding tissue are the same. Heat diffusion from the heater takes place simultaneously with the growth of the heater temperature due to light absorption. This process is described well by the heat conduction equation. Figures 3a and 3b show the temperature profiles in the cylindrical target and the surrounding tissue at different instants of time for the rectangular EMR pulse and the rectangular temperature pulse, respectively. Curve 1 in both figures is the temperature profile at the time equal to the thermal relaxation time of the whole target. The latter time is $TRT=d_2^2/16k$. In our case the TRT=27 ms. We can see that at the time instant t=TRT the boundary temperature of the target is still significantly below the damage temperature. Curve 2 in both figures is the temperature profile at the moment when the boundary temperature of the target reaches the damage temperature T_2. At this moment, the whole target becomes damaged but the surrounding tissue is still intact. It is this time that has been defined above as the thermal damage time (TDT). In our case TDT=1.8 s for the rectangular EMR pulse and TDT=360 ms for the rectangular temperature pulse. Based on this example, we can make two main conclusions. First, the ratio TDT/TRT is about 67 and 13 for the rectangular EMR pulse and the rectangular temperature pulse modes, respectively. Therefore, in both modes the pulsewidth τ=TDT is significantly longer than the TRT of the entire target. Second, at the time instant when t=TDT the heated area is significantly larger than the damaged target. These observations present a striking contrast to the classical case of selective photothermolysis. The distinction above is a result of the spatial separation of the heavily pigmented and the treated areas. Actually, in contrast to the classical case, the basic damage mechanism is now heat diffusion rather than direct heating

by EMR absorption. The heat diffusion front is not sharp and, therefore, heat is spreading outside the damaged area; however, the damage is still rather selective.

We have described the difference in treatment modality between uniformly and non-uniformly pigmented targets. The new extended theory of selective thermal damage of non-uniformly pigmented structures in biological tissue postulates the following:

1. The EMR wavelength should be chosen to maximize contrast between the absorption coefficient of the pigmented area and that of the tissue surrounding the target. This postulate is identical to the case of classical selective photothermolysis.
2. The EMR power should be limited to prevent absorption loss in the pigmented area, but it must be sufficient to achieve a heater temperature higher than the target damage temperature.
3. The pulsewidth should be made shorter than or equal to the thermal damage time (TDT), which can be significantly longer than the thermal relaxation time of the target.

2. Treatment parameters for planar, cylindrical and spherical targets

Heat diffusion is strongly dependent on the heater and target geometry. In this section, we discuss three basic geometries: planar, cylindrical and spherical (Fig. 5). In all cases, we assume a heater with size d_1 located in the center of a target with size d_2. We define the ratio $x= d_2/d_1$ to be *the geometrical factor of the target.* As before, T_1 is the maximum pigmented area temperature, and T_2 is the target damage temperature ($T_1 > T_2$). As we show in the Appendix, the target thermal damage time can be expressed by the following formula:

$$TDT=TRT\times r(x,\Delta),$$

where $r(x,\Delta)$ is a function of the geometrical factor x and *temperature factor* Δ defined as $\Delta=(T_2- T_0)/(T_1- T_0)$. T_0 is the target and heater temperature before irradiation. Normally T_0 is body temperature and is equal to 37°C. TDT is proportional to the TRT. In the Appendix, we present formulas for the TDT of planar, cylindrical and spherical targets. Figure 6 shows the ratio $r(x,\Delta)$=TDT:TRT as a function of geometrical factor x for two heating modes: rectangular EMR pulse and rectangular temperature pulse. The calculation Parameters were T_1=100°C, T_2=70°C, T_0=37°C (Δ=0.52).

We emphasize that in the framework of our analytic theory, the ratio $r(x,\Delta)$ does not depend on the size of the entire target and the tissue thermal properties. Several important conclusions follow from Figure 6.

First, the ratio TDT/TRT is an increasing function of geometrical factor x.

Second, the actual value of this ratio is very different for plane, cylindrical, and spherical targets. For a plane target, the TDT is several times higher than the TRT. The TDT exhibits appreciable growth with increasing the target dimensionality. It is implied herein that the planar, cylindrical, and spherical targets are one-, two-, and three-dimensional, respectively.

Third, for the same TDT/TRT, the relative size of the damaged zone x is smallest for the spherical target. Next in this order is the cylindrical target. The plane target exhibits the largest damage area. The relative size x of the damaged zone around the heater decreases when increasing the target dimensionality. The latter two conclusions are intuitively apparent. Actually, conductive heating of a weakly absorbing tissue should proceed more effectively for a low-dimensional target. This "dimensionality" concept is a useful target parameter. It is also applicable to non-symmetrical targets. The temperature profile is sharper and better localized for the

spherical heater compared to the cylindrical one and it is better for the cylindrical than the planar heater. For the classical case of selective photothermolysis, the target geometry is not important because thermal damage is confined to the same area as the EMR absorption and direct heating. In our case, thermal damage due to heat diffusion is confined to an area that is distinct from the heater. The dependence of heat diffusion on heater geometry is very strong.

Fourth, the ratio TDT/TRT depends strongly on heating mode. The rectangular EMR pulse mode (Fig. 4a) represents the gentlest heating mode because the heater temperature reaches maximum T_1 at the end of the pulse (Fig. 4b). The ratio TDT/TRT is a maximum for this mode. The rectangular temperature pulse mode (Fig. 4d) represents the most aggressive heating mode because the heater temperature reaches a maximum just after the beginning of the pulse and the maximum heater temperature takes place during the EMR pulse. The ratio TDT/TRT is a minimum for the rectangular temperature pulse mode. As mentioned above the rectangular temperature pulse mode can be realized by using an EMR pulse with a special temporal profile. The initial power density should be very high to raise the heater temperature abruptly (for a time interval on the order of or shorter than the TRT). After the maximum temperature is reached, the power density should undergo a steep fall to prevent overheating. Then, to maintain the heater temperature at the prescribed level (Fig. 4c), the power density should fade gradually to compensate the heat flow out of the heater. The pulse power should be precisely adjusted to keep the heater temperature below the collapse temperature T_1. The power depends on heater absorption and size and the EMR attenuation in tissue (see Appendix B). In reality, it is probably difficult to exactly create these two modes. Thus, the real value of TDT can be between these two extreme cases.

The ratio TDT/TRT depends on the temperature factor $\Delta=(T_2- T_0)/(T_1- T_0)$. Table 1 shows the influence of initial target temperature T_0 and maximum heater temperature T_1. All calculations were done for a cylindrical target with the same size as figure 4 for the rectangular EMR pulse. The TDT increases by a factor of 2.2 by precooling from 37°C to 27°C and decreases by a factor of 3 by preheating to 45°C. The fluence should be changed at the same time. If the heater temperature can reach a high value without losing absorption, the TDT can be significantly reduced. The ratio TDT/TRT is close to two (TDT=2TRT) for the case when the heater temperature is 200-250°C. In biological tissue, such a high temperature can be expected in melanin in the hair shaft or in an artificial chromophore such as carbon. But we must remember that the thermal diffusivity can drop in the tissue surrounding the heater due to water vaporization. So this case is very difficult to predict.

Table 1. Thermal damage time (TDT) as function of temperature factor

Initial temperature T_0, °C	Temperature of heater T_1, °C	Temperature of damage T_2, °C	Temperature factor Δ	TDT/TRT
37	100	70	0.53	67
27(precooling)	100	70	0.59	150
45(preheating)	100	70	0.45	22
37	200	70	0.21	2.5
37	240	70	0.17	1.8

As we have shown above, heat diffusion from the heater is very different for different target geometries. The heater temperature should depend on the heater geometry. Figure 7 shows the heater center temperature as a function of pulsewidth for a rectangular EMR pulse with the same power. Spherical, cylindrical, and planar heaters have equal: size d_1, thermal properties, and EMR absorption coefficient. The thermal relaxation time of the heater τ_r depends on geometry, and the ratio is 1:2:3 for spherical, cylindrical, and planar heaters, respectively. If the pulsewidth τ is

significantly shorter than the thermal relaxation time of the heater τ_r ($\tau << \tau_r$) the temperature rises of all the heaters exhibit the same elevation of temperature. However, as shown in Figure 6, the temperature behavior of heaters with different geometries is very different for pulsewidth equal to or longer than τ_r. A steady state heater temperature for a rectangular EMR pulse is possible only for a spherical heater. For cylindrical and especially for planar heaters, the temperature is continuously rising when the pulsewidth is increasing (the power density should be constant, the energy density should be proportional to the pulsewidth). This is because 3D heat diffusion from the spherical heater (in contrast with 2D and 1D heat diffusion from the cylindrical and planar heaters respectively) can compensate constant heating from the rectangular EMR pulse. This phenomenon is very important for uniform targets when the heater and target are the same. For example, the temperature of epidermis (planar target) for a rectangular optical pulse at a wavelength strongly absorbed by melanin will continuously rise during a long pulse ($\tau >> \tau_r$). However, for a spherical target such as the hair bulb matrix, the temperature will stabilize at a steady-state level. To produce a constant heater temperature (rectangular temperature pulse as shown in Figure 4d, the EMR pulse shape must be special (Fig. 4c) with a strong peak in the beginning and decaying amplitude. The ratio of peak and decaying amplitudes are different for heaters with planar, cylinder and spherical geometries (Fig. 8)

3. Mechanism of selective damage of high density targets by heat diffusion.

Since the results obtained in the above sections were presented just for isolated targets, it is important to see the effect of high-density targets. As shown above, non-pigmented targets located close to pigmented areas can be destroyed by heat diffusion. However, heat flux will leak out of the target and the heating area will

be larger than the target. This increases the risk of overheating the tissue surrounding the target and thus the risk of unselective damage. Very roughly the fluence to produce unselective bulk tissue damage F_{NS} is $(d_3/d_2)^n$ times higher than the fluence required to produce selective damage F_S, where d_2 and d_3 are the target size and distance between target centers, and n is 1,2 or 3 for planar, cylindrical, and spherical targets, respectively. So as a first approximation, F_{NS}/F_S is proportional to the ratio of target volume and tissue bulk volume and is independent of pulsewidth. The risk of unselective damage increases in the following order: spherical, cylindrical and planar targets.

More precisely, consider this problem for the ideal model of cylindrical targets with equal spacing. Figures 9 shows the dependence of TDT, F_S, and F_{NS} on *density factor* $y \equiv d_3/d_2$ for a rectangular temperature pulse. As seen from Figure 9, F_S decreases in y beginning with y=4. This effect is explained by the influence of heat fluxes from neighboring targets. But at the same time, the F_{NS} is continuously dropping as function of density factor y. So for y<4 the range of safe fluences is going to be very narrow and the risk of unselective damage will increase. In the case of short pulse/high-power irradiation where the chromophore is ablated, the energy delivered to the tissue is therefore limited. This provides additional protection in the case of high-density target treatment.

4. Applications of the extended theory of selective photothermolysis

Now we are going to discuss applications of the new theory. Thus far, we have considered at some length the method of selective photodamage of unpigmented targets in the tissue. We will present two examples where the new theory can be applied: photoepilation and photosclerotherapy.

Photoepilation. Photoepilation utilizes light to cause thermal or mechanical damage of hair follicles. To achieve hair growth delay, it is sufficient to either damage matrix cells of anagen hair follicles or coagulate blood vessels of the papilla or possibly to destroy part of the outer root sheath [2]. For permanent hair-follicle damage, in accordance with current knowledge, it is necessary to damage stem cells that are located in the bulge area at the interface of the outer root sheath and the connective tissue sheath [6]. One can also irreversibly damage a hair follicle at the level of the dermis by replacing it with connective tissue.

The matrix cells produce the hair shaft. The matrix cells contain melanosomes that produce hair melanin. The concentration of melanin in the matrix cells is significantly higher than in the hair shaft. Melanin is distributed uniformly and densely in the matrix cells. So for a pulsewidth longer than the TRT of individual melanosomes (1μs), the matrix cells act as a uniformly pigmented target. This is a typical example of a target where standard selective photothermolysis theory is applicable. For selective and effective treatment, the energy and pulsewidth have to be significantly shorter than the TRT of the matrix cells. The matrix cells form a dome shaped structure with the smallest cells close to half of the hair shaft diameter d_h. So the TRT of the hair matrix can be estimated as the TRT of a layer with thickness $d_h/2$, that is $d_h^2/32k$. The pulsewidth values for effective treatment are presented in Table 2.

Table 2. Optimum pulsewidth for hair-follicle treatment.

Hair type/diameter	TRT of hair shaft, ms	TRT of hair follicle, ms	Halting hair shaft growth			Permanent hair-follicle destruction	
			TRT of hair matrix, ms	TDT of papilla blood vessel, ms		TDT of stem cell, ms	
				Rectangular temperature pulse	Rectangular light pulse	Rectangular temperature pulse	Rectangular light pulse
Fine/30μ	0.6	5.4	<0.3	0.5	1.5	30	115
Medium coarse/70μ	3	27	<2	2.7	8.5	170	610
Large coarse/120μ	9.6	87	<5	8	21	510	1800

Another method of halting hair shaft growth is to coagulate blood vessels in the papilla. The loop of blood vessels in the papilla is located in the center of the matrix cell dome. Blood absorption is significantly lower than melanin absorption in the neighboring matrix cells because of the small vessel size. So the most effective method of papilla blood vessel coagulation is to utilize heat diffusion from the matrix cells that absorb light. This is a typical case where the extended theory of selective photothermolysis can be applied. The highly pigmented heater (the matrix cells) and the lightly pigmented target (the blood vessels) are separated by distance about $d_h/2$. We calculated the TDT of the hair papilla blood vessels using our thermal diffusion model assuming the maximum heater temperature to be T_1=100°C and the blood vessel coagulation temperature to be T_2=65°C. The TDT value for different hair sizes and heating modes are presented in Table 1. We can see a significant difference in optimum treatment pulsewidth for: 1) the matrix cells by direct light absorption and 2) the papilla blood vessel loop by heat diffusion.

Let us now consider damage of hair stem cells. They are located in the basal cell layer of the outer root sheath of the lower isthmus. The stem cells do not have any pigment that can effectively absorb light in the therapeutic window (600-1200

nm), which is also the best wavelength range for photoepilation [2]. However, the stem cells can be damaged by heat diffusion from the melanin-rich hair shaft or an artificial chromophore inside the inner root sheath. This case is very well described by the cylindrical model that we considered in some detail above. The optimum treatment pulsewidth of the stem cells is close to the TDT of the follicle structure. If we assume that the maximum hair-shaft temperature is T_1=100°C and the damage temperature of the stem cells is T_1=65°C, we can calculate the TDT as shown in Table B (approximate formulas give us slightly lower values than the exact modeling we presented in Figure 6b). Calculation results for a follicle with a ratio of follicle diameter to hair-shaft diameter of x=3 are presented in Table 2.

To estimate power density P and fluence F for the rectangular light pulse case, we can use formulas from Table 2A (See Appendix) that we can simplify for the follicle case as:

$$P = \frac{32}{\mu_a q} \cdot \frac{x^2}{\mathrm{TRT}} \cdot \frac{T_1 - T_0}{\ln\left(1.4x^2 \cdot \frac{\mathrm{TDT}}{\mathrm{TRT}}\right)} [W/cm^2]$$

$$F = P \cdot TDT [J/cm^2]$$

where $\mu_a[cm^{-1}]$ is the hair-shaft absorption coefficient, q is the ratio of the radiance at the target location to the input power density (attenuation factor). For our calculation, we use typical treatment conditions: wavelength is 800 nm, dark hair with μ_a=100 cm^{-1}, x=3, q=1(low isthmus level of follicle), T_1=100°C , T_2=65°C, and T_0=36°C. Using the formulas shown above, we calculate the following values: power density is 560

W/cm^2 for 30 μm fine hair, 100 W/cm^2 for 70 μm terminal hair and 35 W/cm^2 for 120 μm coarse hair. For these hairs with equal melanin concentration and different diameters, the fluence necessary to damage the stem cells is the same. The fluence value is 40 J/cm^2. The pulsewidth value appears in Table 2 as the TDT for a rectangular light pulse. We can see from Table 2 that selective and complete hair-follicle damage can be achieved over a very broad range of pulsewidths. For example, for a hair shaft diameter of approximately d_1=70 μm and a hair follicle diameter of d_1=210 μm, this range is 170-610 ms, which is significantly longer than the TRT (27 ms). In our in vitro experiment, we observed nearly complete damage of similar size follicles for pulsewidths in the 30-400 ms range with an identical fluence of 35 J/cm^2. The main differences between theory and experiment for short pulses can be explained by differences in the maximum hair-shaft temperature used in the theoretical model (T_1 =100°C) and the hair-shaft temperature reached in the experiment. For a pulsewidth shorter than 100 ms, we saw a significant change in the hair-shaft structure. This implies that the hair-shaft temperature was higher than 250°C. For this temperature the TDT is very close to the TRT (see Table 1). If the energy of the ablation products is not too high, most of them release their energy inside the hair follicle and heat up the follicle structure. So all the absorbed energy was utilized to heat the follicle structure (including IRS and ORS). For a pulsewidth significantly shorter than 30 ms with the same fluence, we can expect more hair-shaft ablation and escape of the hair-shaft ablation products from the hair follicle. In this case, the damaged volume of the hair follicle should decrease with decreasing pulsewidth and, for very short pulses, it should be limited to the hair shaft. The differences between theory and experiment for pulses longer than 400 ms can be

explained by the low power density (<100 W/cm^2) of the laser pulse, which was not sufficient to heat the hair shaft close to 100°C.

Photosclerotherapy. Photosclerotherapy produces thermal or mechanical damage of the vessel structure due to light absorption by blood [6]. The blood hemoglobin exhibits selective light absorption over a wide wavelength range. Optimum vessel closure can be achieved by denaturation of the endothelium that is in direct contact with blood. This case is well described by the standard theory of selective photothermolysis[1]. Other authors have suggested that permanent vessel closure requires denaturation of the vessel wall structure including the tunica intima, tunica medula, and tunica adventitia[3]. These structures do not contain any strongly absorbing chromophores and can be damaged by heat diffusion from blood. Therefore, we will apply the extended theory of selective photothermolysis to estimate treatment parameters for different vein sizes. As a first approximation, the vein can be modeled as by a cylinder. However, this is true just for limited constrained cases depending on the light wavelength and vein size. The cylindrical model is valid if the light penetration depth in the blood exceeds the vessel internal diameter D. In this case, the blood is heated uniformly. If scattering of the blood is lower than absorption, the light penetration depth is roughly equal to the inverse blood absorption coefficient $1/\mu_a$. Thus the cylindrical model can be used when $D<1/\mu_a$. In this case, the heater diameter is $d_1=D$ and the target diameter is $d_2=D+2w$, where w is the vessel-wall thickness. If $D>>1/\mu_a$, the heated zone is a cylindrical blood layer, in contact with the vessel wall. The heated-zone thickness is approximately equal tot the penetration depth $1/\mu_a$. This case can be roughly described by the planar model with heater thickness $d_1=1/\mu_a$ and target thickness d_2.

$=1/\mu_a+2w$. Analytic evaluation of the TDT using the expressions of Table 2A is possible in the rectangular light-pulse case when the whole blood volume is uniformly irradiated. If this is the case the cylindrical target model is applicable. In the opposite limiting case of very strong blood absorption, a thin layer of blood adjacent to the vessel wall is only irradiated. In the latter case one may apply the planar model. At that, the analytic and numeric results show rather good agreement. In other cases both the TDT and the input flux were evaluated numerically. The maximum heater temperature is T_1=100°C (limited by blood coagulation and vaporization), vessel wall denaturation temperature is T_2=65°C, and the initial body temperature is T_0=37°C. The calculations were performed for two wavelengths λ: λ=577 nm (maximum hemoglobin absorption), where $1/\mu_a$=43 μm and moderate hemoglobin absorption λ=1060 nm, where $1/\mu_a$=1400 μm [8,9]. To estimate the power density and fluence for a rectangular light pulse, we can use formulas from Table B and direct modeling for a rectangular temperature pulse. Calculation results for different types of spider veins are presented in Table 3.

Table 3. Optimum pulsewidth for treatment of spider veins.

Diameter of vein, mm	Wall thickness, mm	TRT of blood volume, ms	TRT of vein, ms	TDT of vein and fluence F							
				λ=577 nm				λ=1060 nm*			
				Rectangular temperature pulse		Rectangular light pulse		Rectangular temperature pulse		Rectangular light pulse	
				TDT, ms	F, J/cm²	TDT, ms	F, J/cm²	TDT, ms	F, J/cm²	TDT, ms	F, J/cm²
0.1	0.035	0.5	5	40	10	130	20	40	590	140	1090
0.25	0.08	4	35	150	6	515	15	150	335	610	615
0.5	0.12	35	135	215	4	740	6	215	115	1200	200
1	0.15	260	540	240	4	670	5	240	50	2400	90

* We can predict that TDT and F will be on the same order for another important wavelength (λ=800 nm) because the absorption coefficients for vein blood at λ=800 nm and λ=1060 nm are similar.

As we see from Table 3, the TDT of the entire vein wall structure is shorter for the 577-nm wavelength that coincides with the strong hemoglobin absorption peak. The TDT can be very long, typically for large veins. The perfusion factor can also be important but is neglected in the present study. Blocking of the blood flow can be important for optimum treatment with such a super long pulse. The large veins need significantlt lower fluence, power density, and longer pulsewidth than small veins. This dependence is even stronger for light with low absorption in hemoglobin. The water absorption of surrounding tissue can be important for long treatment wavelengths (λ>750nm) due to parallel non-selective heating by water absorption that can increase the tissue temperature T_0. As we showed above, the TDT will be shorter in this case and the fluence will be lower.

The parameters for spider-vein treatment suggested by our new theory are very different compared to typical clinical parameters used for photosclerotherapy and should be clinically proven.

Following from tables 2 and 3, the treatment time (pulsewidth) for hair follicles and spider veins is on the order of several hundreds of milliseconds. As was showed in [10], parallel cooling of the epidermis (simultaneous heating by light absorption and heat removal by heat diffusion into the skin and cooling agent) is very effective in this pulsewidth range. This cooling mode is important for epidermal protection and makes the procedure more effective because high fluence can be delivered through the epidermis.

Conclusions

1. Our in vitro experiment demonstrated that the hair-follicle damage pattern for fixed fluence is selective and pulsewidth independent over a broad pulsewidth range; this range is 1-10 times the hair-follicle TRT.
2. A new theory of selective thermal damage of non-uniformly pigmented structures of biological tissues is presented in this paper. We call this theory the extended theory of selective photothermolysis (ESP).
3. The extended theory of selective photothermolysis is important for biological targets with space between all or part of the target and the pigmented area of the tissue. So, in contrast with the standard theory of selective photothermolysis the target is destroyed by heat diffusion from the pigmented area to the target but not by direct heating from electromagnetic radiation (EMR).
4. The main principles of the extended theory of selective photothermolysis are:
   - The EMR wavelength should be chosen to maximize contrast between the absorption coefficient of the pigmented area and that of the tissue surrounding the target. This postulate is identical to the case of classical selective photothermolysis.
   - The EMR power should be limited to prevent absorption loss in the pigmented area, but it must be sufficient to achieve a temperature of the pigmented area higher than the target damage temperature.
   - The pulsewidth should be made shorter than or equal to the thermal damage time (TDT). The TDT is the time required for irreversible target damage with sparing of

the surrounding tissue. The TDT can be significantly longer than the thermal relaxation time (TRT) of the entire target.

5. The power and shape of the EMR pulse are important for successful treatment in contrast with the standard theory of selective photothermolysis where just fluence is important.
6. Treatment parameters are power and pulsewidth dependent and are not just dependent on target size, absorption and thermal properties but their geometry as well.
7. For highly dense targets, it is important to limit fluence to prevent non-selective damage. Selective treatment of very high density targets is not possible because the gap between the fluence of selective and non-selective treatment is too small.
8. The extended theory of selective photothermolysis suggests a significantly longer treatment time (pulsewidth) than classical selective photothermolysis. In dermatology, it provides the additional benefit of epidermal protection due to parallel cooling.
9. The extended theory of selective photothermolysis presented in this paper is useful for electrothermolysis (electrode is heater) and certain cases of magnetic and acoustic treatment of tissue.

Appendix.

Procedure to determine the amplitude and the duration of the rectangular EMR pulse: brief summary.

The present Appendix summarizes the EMR pulse parameters for the treatment of the basic targets exhibiting a high degree of symmetry, i.e., the planar, cylindrical, and spherical ones.

The notations and the basic parameters of the problem are explained in Table 1A:

Table A1

Variable	Dimensionality	Name	Assumptions and relations
k	$cm^2\ s^{-1}$	Thermal diffusivity	Assumed to be the same all over the target
ρ	$g\ cm^{-3}$	Density	Assumed to be the same all over the target
c	$J/(g\ ^0K)$	Specific heat	Assumed to be the same all over the target
μ_a	cm^{-1}	Tissue absorption coefficient	Assumed to be zero outside the heater
q	a.u.	The ratio of radiance to the input power density	
d_1	Cm	Thickness or diameter of the heater	
d_2	Cm	Thickness or diameter of the target	$d_2 > d_1$
d_3	Cm	Mean spacing between the targets	$d_3 > d_2$
T_0	^0C	Initial temperature of both the target and the surrounding tissue	$T_0 = 37^0 C$
T_{1max}	^0C	Temperature of heater absorption loss, collapse temperature	$T_{1\max} = 100^0 C - 250^0 C$
T_1	^0C	Maximum temperature of the heater(absorber)	$T_2 < T_1 \le T_{1\max}$
T_2	^0C	Temperature of irreversible damage of the tissue	$T_2 = 70^0 C$
Δ	a.u.	Temperature factor, temperature ratio	$\Delta \equiv \frac{T_2 - T_0}{T_1 - T_0} < 1$
x	a.u.	Geometrical factor, diameter ratio	$x \equiv d_2/d_1 > 1$

Our analysis was based on the heat conduction equation. We have found approximate analytic solutions of thermal damage time (TDT) and input power density P.

The final expressions for the important variables in question are outlined in simplified form in Table 2A below. It is implied that the thermal constants, i.e., the density, the thermal diffusivity, and the thermal conductivity do not vary significantly within the target and the surrounding tissues.

Table 2A

N	Quantity	Notation [Dimensionality]	Approximate expression for a particular target geometry: Planar	Cylindrical	Spherical
1	Thermal relaxation time of the heater	τ_r [s]	$\tau_r = \frac{d_1^2}{8 \cdot k}$	$\tau_r = \frac{d_1^2}{16 \cdot k}$	$\tau_r = \frac{d_1^2}{24 \cdot k}$
2	Thermal relaxation time of the target	TRT [s]	$TRT = \frac{d_2^2}{8 \cdot k} = x^2 \cdot \tau_r$	$TRT = \frac{d_2^2}{16 \cdot k} = x^2 \cdot \tau_r$	$TRT = \frac{d_2^2}{24 \cdot k} = x^2 \cdot \tau_r$
3	Thermal damage time	TDT [s]	$TDT = \frac{TRT}{2 \cdot x^2} \cdot \left[\left(\frac{D-\Delta}{1-\Delta}\right)^2 - 1\right]$, $D = \exp(-x^2) + 1.8 \cdot x \cdot \mathrm{erf}(x)$.	$TDT = \frac{TRT}{x^2} \cdot \exp\left(\frac{D-0.3\cdot\Delta}{1-\Delta}\right)$, $D = 0.6 + 2 \cdot \ln(x) - \mathrm{Ei}(-1.4 \cdot x^2)$	$TDT = \begin{cases} 0.9 \cdot \frac{TRT}{x_t^2}\left[\left(\frac{1-\Delta}{D-\Delta}\right)^2 - 1\right], & D-\Delta > 0 \\ \infty, & D-\Delta \le 0. \end{cases}$ $D = 0.7 \cdot \frac{\mathrm{erf}(1.3 \cdot x)}{x}$.
4	Input power density	P [W/cm^2]	$P = \frac{\rho \cdot c}{\mu_a q} \cdot \frac{1.1 \cdot x^2}{TRT} \cdot \frac{T_1 - T_0}{\sqrt{1 + 2.1 \cdot x^2 \cdot \frac{TDT}{TRT}} - 1}$	$P = \frac{\rho \cdot c}{\mu_a q} \cdot \frac{x^2}{TRT} \cdot \frac{T_1 - T_0}{\ln\left(1 + 1.4 \cdot x^2 \cdot \frac{TDT}{TRT}\right)}$	$P = \frac{\rho \cdot c}{\mu q} \cdot \frac{0.3 \cdot x^2}{TRT} \cdot \frac{T_1 - T_0}{1 - \frac{1}{\sqrt{1 + 1.2 \cdot x^2 \cdot \frac{TDT}{TRT}}}}$
5	Input fluence	F [J/cm^2]	$F = P \cdot TDT$	$F = P \cdot TDT$	$F = P \cdot TDT$

The present discussion is restricted to rectangular EMR pulses only. Our goal herewith is to determine the pulsewidth and the pulse amplitude. This may be performed in the following order:

1. Based on the target geometry, the size of the pigmented area (heater) d_1, size of the target d_2, distance between targets d_3, the geometrical factor $x = d_2/d_1$ and density factor can be determined.

2. Based on the thermal properties of the target and chromophore, the temperature of pigmented area absorption loss T_{1max}, temperature of target damage T_2, initial tissue temperature T_0, the temperature factor $\Delta=(T_2- T_0) /(T_1- T_0)$ can be determined.

3. Using these parameters and formulas, we can use the formulas in Table 2A, rows 1-3 to determine τ_r, TRT and finally TDT. As explained above, the TDT is approximately equal to the optimum duration of the EMR pulse τ_0.

4. Based upon an estimate of the EMR attenuation factor at the depth of target q and the absorption coefficient of pigmented area μ_a and the heater temperature T_1, the power density on the skin P using can be determined by using the formulas from Table 2A row 4. The power density should be limited in order to not bleach the pigmented area, but it should be significantly high to rich the temperature of target damage T_2.

5. Treatment fluence is given by $F = P \cdot \mathrm{TDT}$ or $F = P \cdot \tau_0$

In contrast to both the planar and cylindrical targets, the TDT for the spherical target may be evaluated to infinity (see Table 2A, row 3, rightmost column). This means that one cannot ensure the safety of the heater in an attempt to damage the whole target. After a part of the target becomes damaged, the heater temperature reaches the crucial value T_1. This gives rise to phase transitions, bleaching, bubble formation, and other nonlinear processes lying outside the scope of this paper. Therefore, our simple theory provides the means to describe thermal damage of sufficiently small spherical targets only. More precisely, for a given value of Δ the

diameter ratio x must not exceed the value obtained from the equation $D = 0$, where variable D is a function of x determined by the last expression of Table 2A, row 3, rightmost column.

Figures.

Figure 1. Thermal damage pattern of hair follicle (HF) at bulge level demonstrated by loss of LDH activity, Fluence was 35 J/cm^2. Bar, 100 μm. There is selective damage of the hair follicle over a wide range of pulsewidths, and the extent of thermal damage does depend on hair-shaft diameter and pigmentation. (a) τ= 30 ms, I= 1170 W/cm^2. Right HF demonstrates almost complete damage of outer root sheath (ORS), hair shaft (HS) structurally disintegrated with browning, fragments of HS partly protruded through ruptured IRS, no perifollicular damage. Left HF presents vacuoles within HS, no browning, IRS ruptured, partial loss of LDH activity of ORS and no perifollicular damage. Middle HF with fine and light pigmented HS does not demonstrate any HS alteration or loss of LDH activity. (b) τ= 100 ms, I= 350 W/cm^2. Right HF without any HS alteration or loss of LDH activity of ORS. Left HF with vacuoles within HS, IRS ruptured, loss of LDH stain of entire ORS and a thin cuff of perifollicular tissue. (c) τ= 200 ms, I=175 W/cm^2. No hair shaft alterations for both HF. Right HF with minor loss of LDH activity of ORS. Left HF with partial loss of LDH activity of ORS. No perifollicular damage. (d) τ= 200 ms, I=175 W/cm^2. No hair shaft alterations for both HF. Right HF with partial loss of LDH activity of ORS. Left HF with complete loss of LDH activity of ORS. Interfollicular damage of these adjacent HF

with only 300 μm interfollicular distance. Note more pronounced pigmentation of hair shafts than in fig. 1c. (e) τ= 350 ms, I=100 W/cm^2. No hair shaft alterations for both HF, IRS not damaged, partial loss of LDH activity for both HF, more pronounced loss for HF with more pigmented HS.

Figure 2. General structure of biological target with space separation between target and absorber (heater).

Figure 3. Temperature distribution in the tissue with cylindrical absorber with diameter 0.07 mm and target with diameter 0.21 mm. Figure 3a shows the temperature distribution for a rectangular EMR pulse at two points in time: bottom curve at t=TRT=27.5ms and top curve at t=TDT=1.6s. Figure 3b shows the temperature distribution for a rectangular temperature pulse at two points in time: bottom curve at t=TRT=27.5ms and top curve at t=TDT=0.36s. Maximum temperature of the absorber is T_1 =100°C. Damage temperature is T_2 =70°C. Initial temperature is T_0 =37°C. The absorption of surrounding heater tissue was neglected.

Figure 4. Time dependence of electromagnetic radiation (EMR) power and temperature of the heater (absorber). Two basic cases are shown: (Fig. 4a) rectangular EMR pulse and (Fig. 4c) rectangular temperature pulse. Figure 4b shows heater temperature as a function of time that is produced by a rectangular EMR pulse. Figure 4d shows EMR power as function of time that produces a rectangular temperature pulse at the heater.

Figure 5. Three types of target with different geometry: (a) planar, (b) cylindrical, (c) spherical. 1 is the heater (absorber). 2 is the target. d_1 is size of the heater, d_2 is size of the target.

Figure 6. The ratio r of thermal damage time (TDT) and thermal relaxation time (TRT) as function of ratio x of size of the target d_2 and size of the heater d_1 for different target geometries: (Figure 6a) planar, (Figure 6b) cylindrical, (Figure 6c) spherical. Ratio r=TDT:TRT is given for two heating modes: rectangular EMR pulse and rectangular temperature pulse.

Figure 7. Increase of heater temperature T(t) normalized to steady state and temperature of spherical heater increase T_0 as a function of heating time for rectangular pulse and different type of heaters with the same size: (1) planar, (2) cylinder and (3) sphere.

Figure 8. EMR power P(t) pulses producing rectangular temperature pulse on the heater normalized to peak power P_0 at t=0 for different target geometries with the same size: (1) planar, (2) cylinder and (3) sphere.

Figure 9. Thermal damage time and damage fluence for high density targets as a function of density factor y (ratio of distance between centers of targets d_3 and size of the target d_2). Figure 9a shows the dependence of TDT for selective (bottom curve) and nonselective (top curve) damage on density factor y. Figure 9b shows dependence of damage fluence for selective F_S (bottom curve) and nonselective F_{NS} (top curve) damage on density factor y. Both curves are normalized to the damage

fluence of individual target F_0. Calculations were done for a cylindrical individual target with parameters the same as those used for Figure 3.

Figure A1. Heat production as a function of radius. The approximation of the stepwise function distribution (solid curve) by the Gaussian distribution (dotted curve).

References

1. Anderson RR, Parrish J. Selective photothermolysis: Precise microsurgery by selective absorption of the pulsed radiation. Science 1983; 220: 524-526.
2. Dierickx CC, Grossman MC, Farinelli WA, Anderson RR. Permanent hair removal by normal-mode ruby laser. Arch Dermatol 1998; 134:837-842.
3. Neumann RA, Knobler RM, Leonhartsberger H, Gebhart W. Comparative histochemistry of port-wine stains after copper vapor laser (578nm) and argon laser treatment. J Invest Dermatol 1992; 99(2): 160-167
4. Balogh K Jr, Dudley HR, Cohen RB. Oxidative enzyme activity in skeletal cartilage and bone. A histochemical study. Lab Invest 1961; 10: 839-845
5. Henriques FC, Moritz AR. Studies of thermal injury. I. The relative importance of time and surface temperature in the causation of cutaneous burns. Amer. J. Pathol. 1947; 23: 695-720.
6. Sun T, Cotsarelis G, Lavker RM. Hair follicle stem cells: the bulge activation hypothesis. J Invest Dermatol 1991; 96(suppl 5):77S-78S.
7. Dover JS, Amdt KA. New approaches to the treatment of vascular lesions. Lasers Surg Med 2000;26:158-163.
8. Roggan A, Friebel M, Doershel K, Hahn A, Mueller G. Optical properties of circulating human blood in the wavelength range 400–2500 nm. J. Biomedical Optics 1999; 4:36-46.

9. Yaroslavsky AN, Yaroslavsky IV, Goldbach T, Schwarzmaier HJ. Optical properties of blood in the near-infrared spectral range. Proc. SPIE 1996; 2678: 314-324.

10. Zenzie HH, Altshuler GB, Smirnov MZ, Anderson RR. Evaluation of cooling methods for laser dermatology. Lasers Surg Med 2000; 26:130-144.

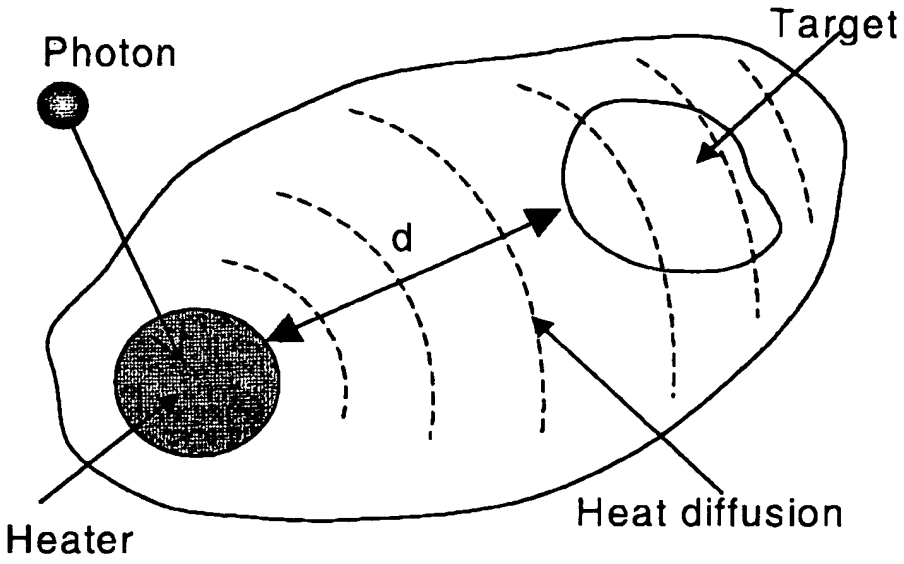

Figure 2.

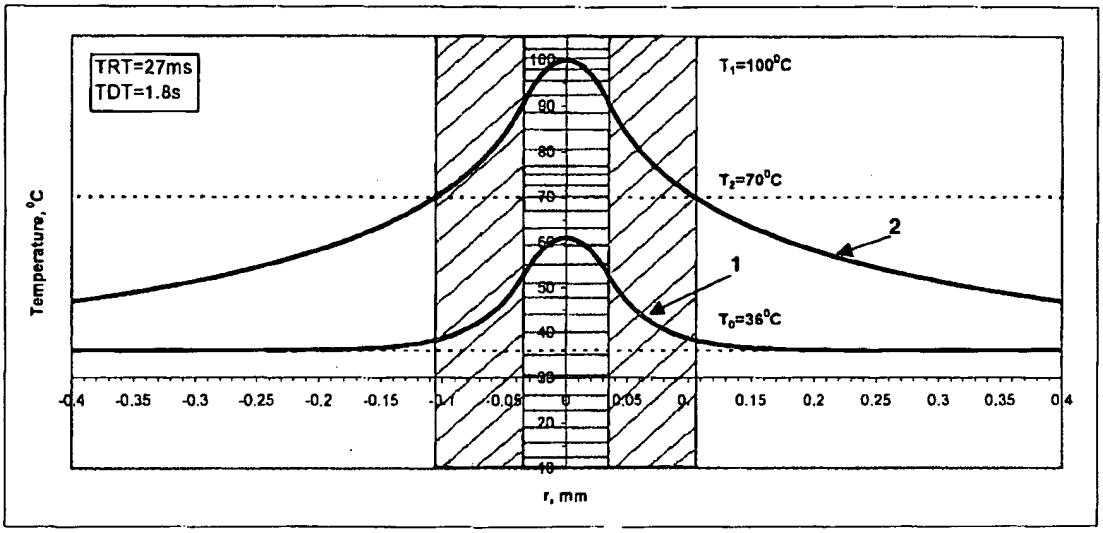
TRT=27ms
TDT=1.8s
T1=100°C
T2=70°C
T0=36°C
1
2
Temperature, °C
r, mm
-0.4
-0.35
-0.3
-0.25
-0.2
-0.15
-0.1
-0.05
0
0.05
0.1
0.15
0.2
0.25
0.3
0.35
0.4
100
90
80
70
60
50
40
30
20
10

Figure 3a.

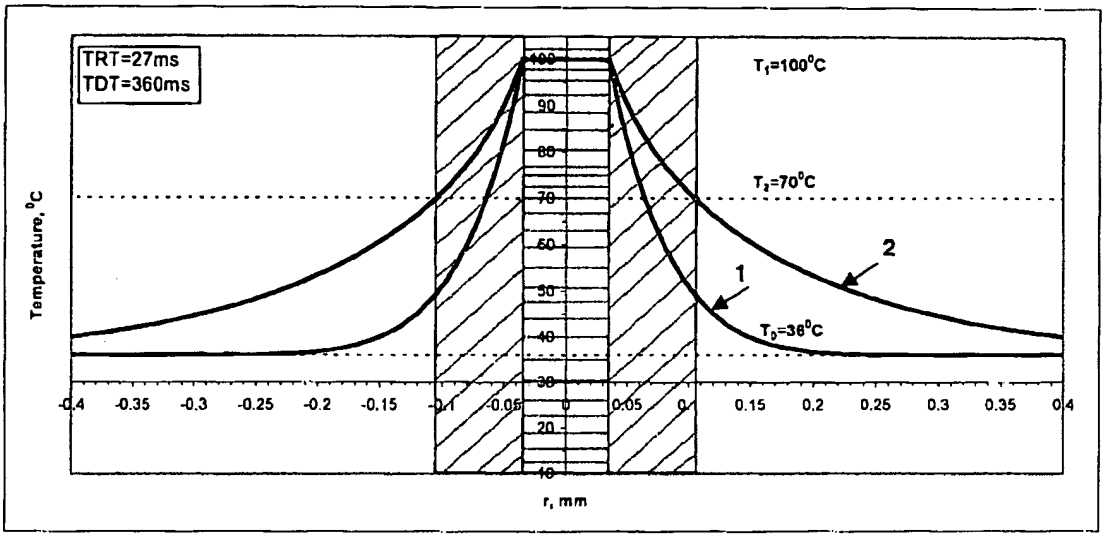
TRT=27ms
TDT=360ms
T_1=100°C
T_2=70°C
T_0=38°C
1
2
Temperature, °C
r, mm
-0.4
-0.35
-0.3
-0.25
-0.2
-0.15
-0.1
-0.05
0
0.05
0.1
0.15
0.2
0.25
0.3
0.35
0.4
90
80
70
60
50
40
30
20
10

Figure 3b.

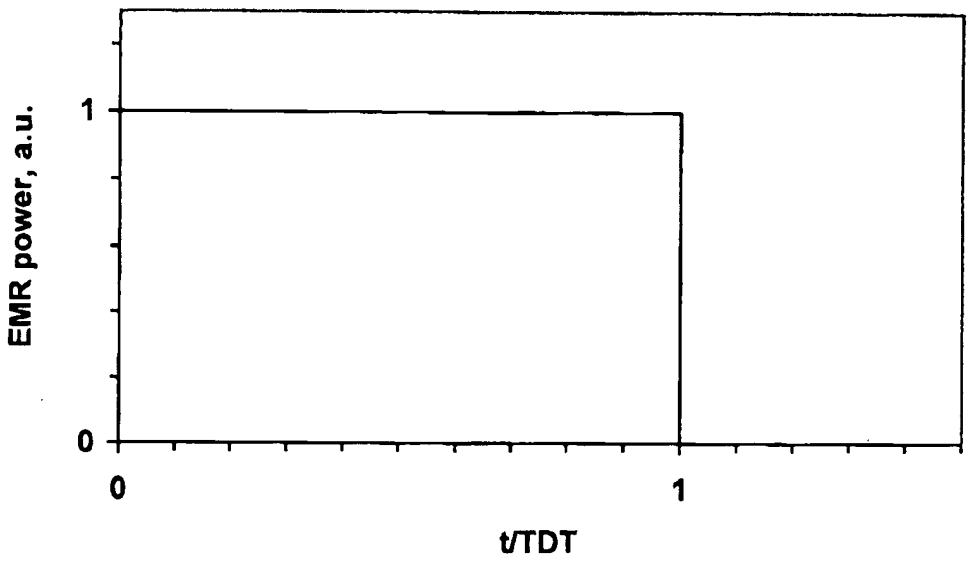

Figure 4a.

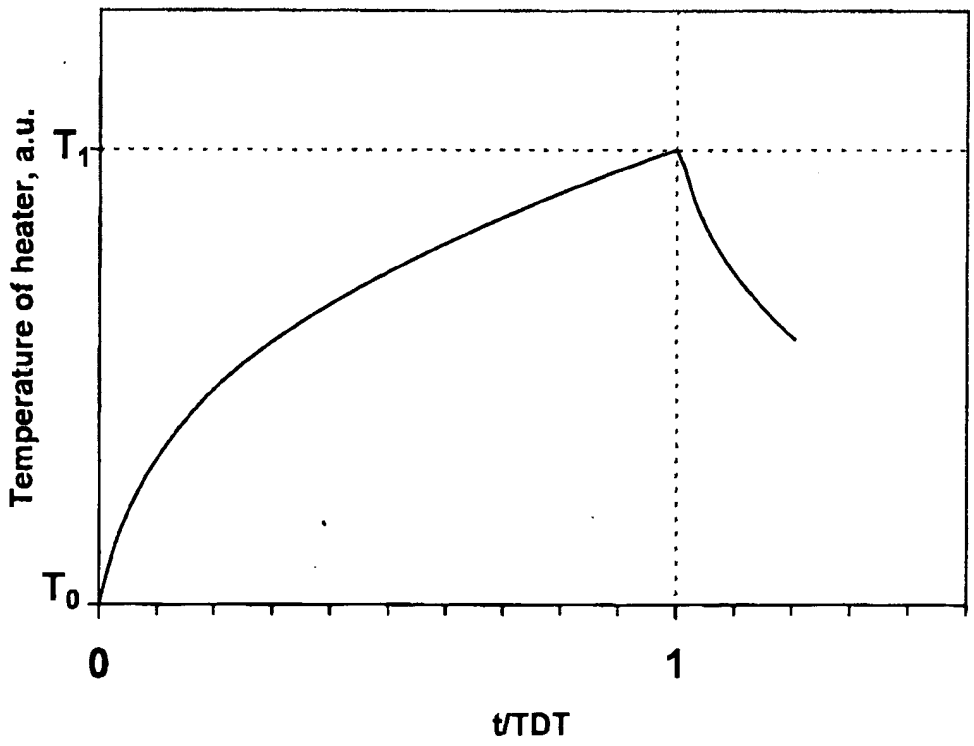

Figure 4b.

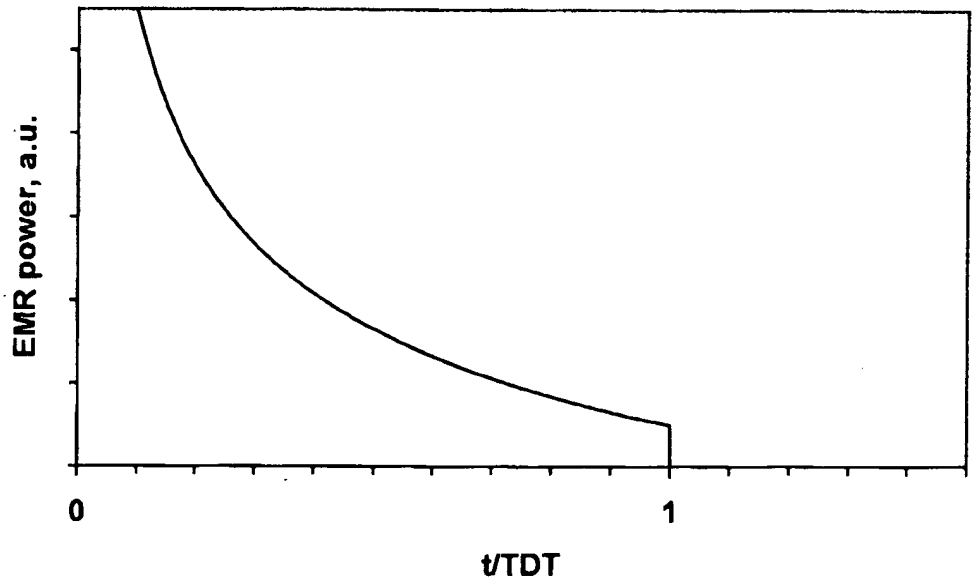

Figure 4c.

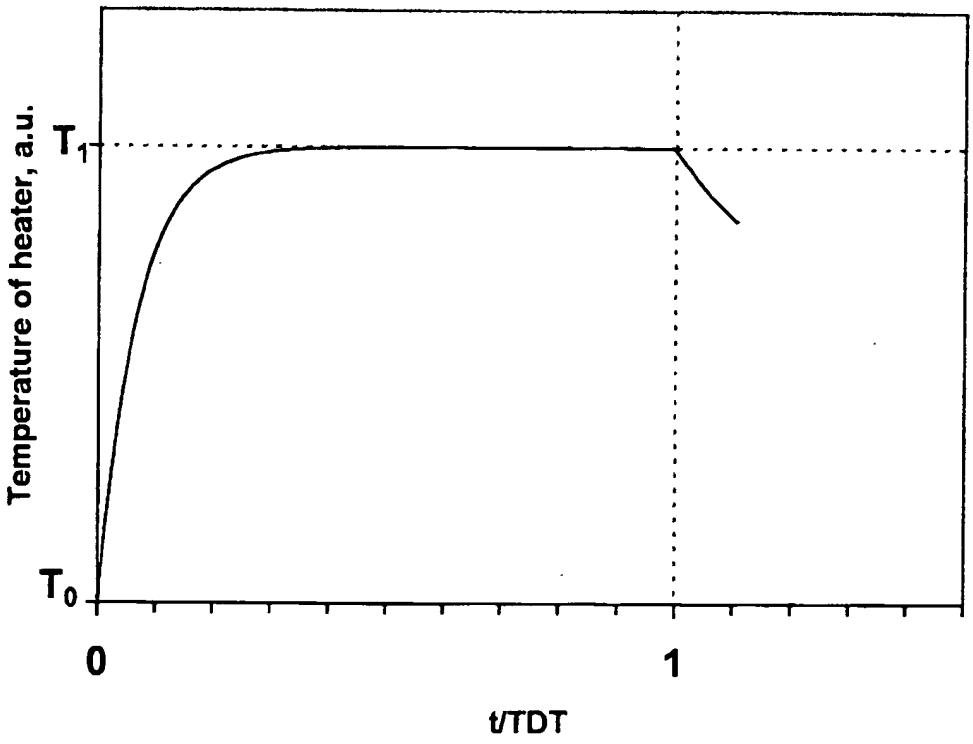

Figure 4d.

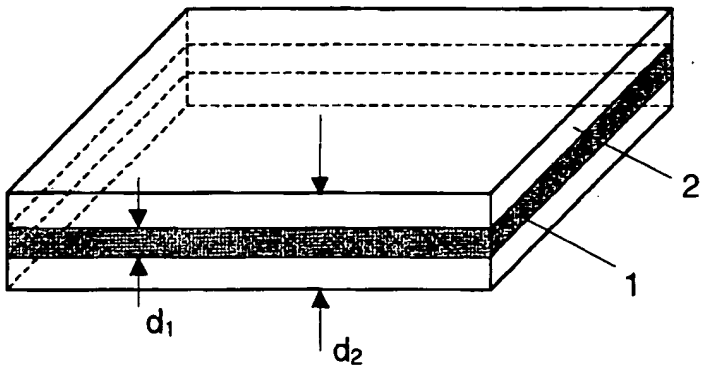

Figure 5a.

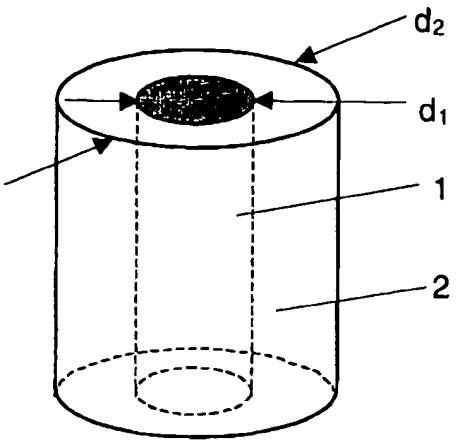

Figure 5b.

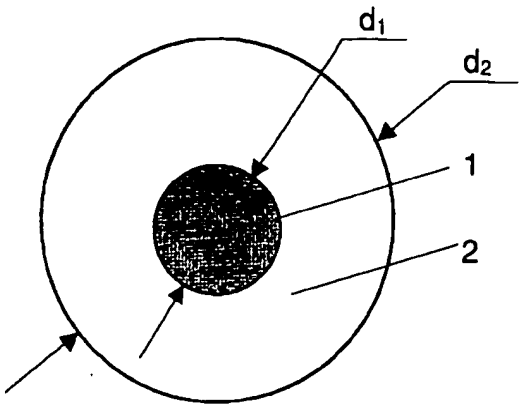

Figure 5c.

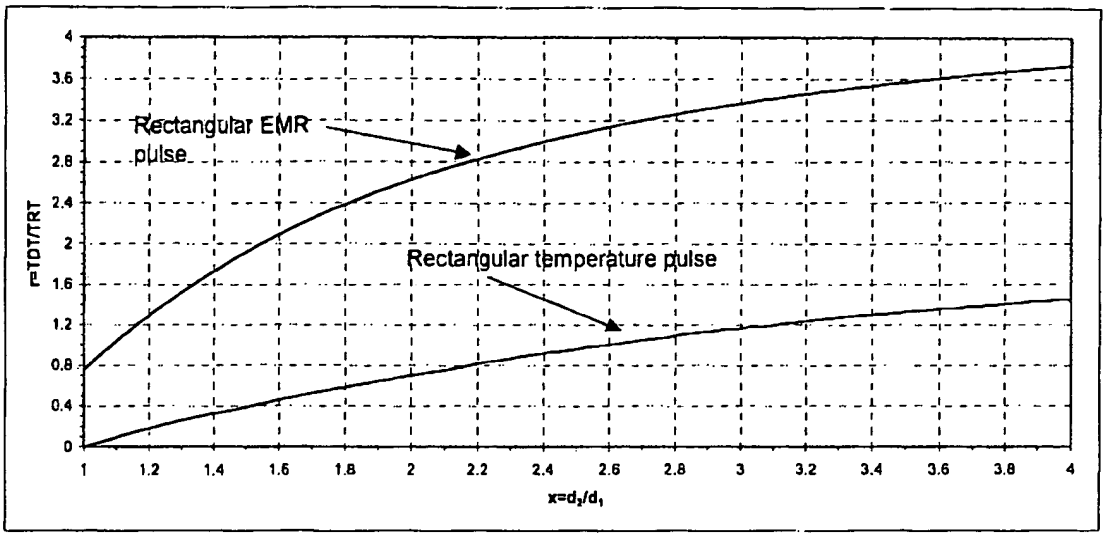
Rectangular EMR pulse
Rectangular temperature pulse
r=T0T/TRT
x=d2/d1
0
0.4
0.8
1.2
1.6
2
2.4
2.8
3.2
3.6
4
1
1.2
1.4
1.6
1.8
2
2.2
2.4
2.6
2.8
3
3.2
3.4
3.6
3.8
4

Figure 6a.

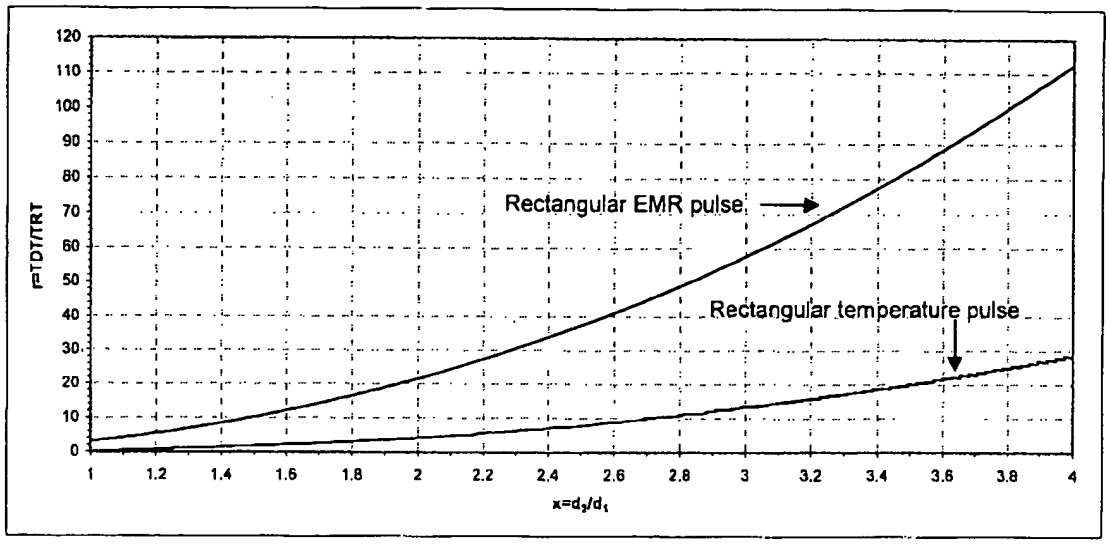
120
110
100
90
80
70
60
50
40
30
20
10
0
r=TDT/TRT
Rectangular EMR pulse
Rectangular temperature pulse
1
1.2
1.4
1.6
1.8
2
2.2
2.4
2.6
2.8
3
3.2
3.4
3.6
3.8
4
x=d2/d1

Figure 6b.

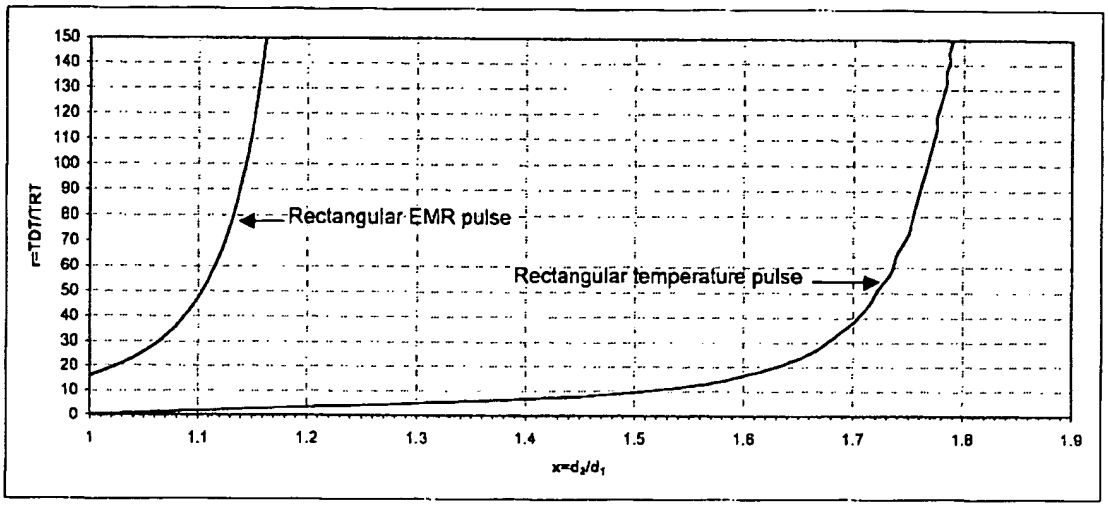
150
140
130
120
110
100
90
80
70
60
50
40
30
20
10
0
r=TDT/TRT
Rectangular EMR pulse
Rectangular temperature pulse
1
1.1
1.2
1.3
1.4
1.5
1.6
1.7
1.8
1.9
x=d2/d1

Figure 6c.

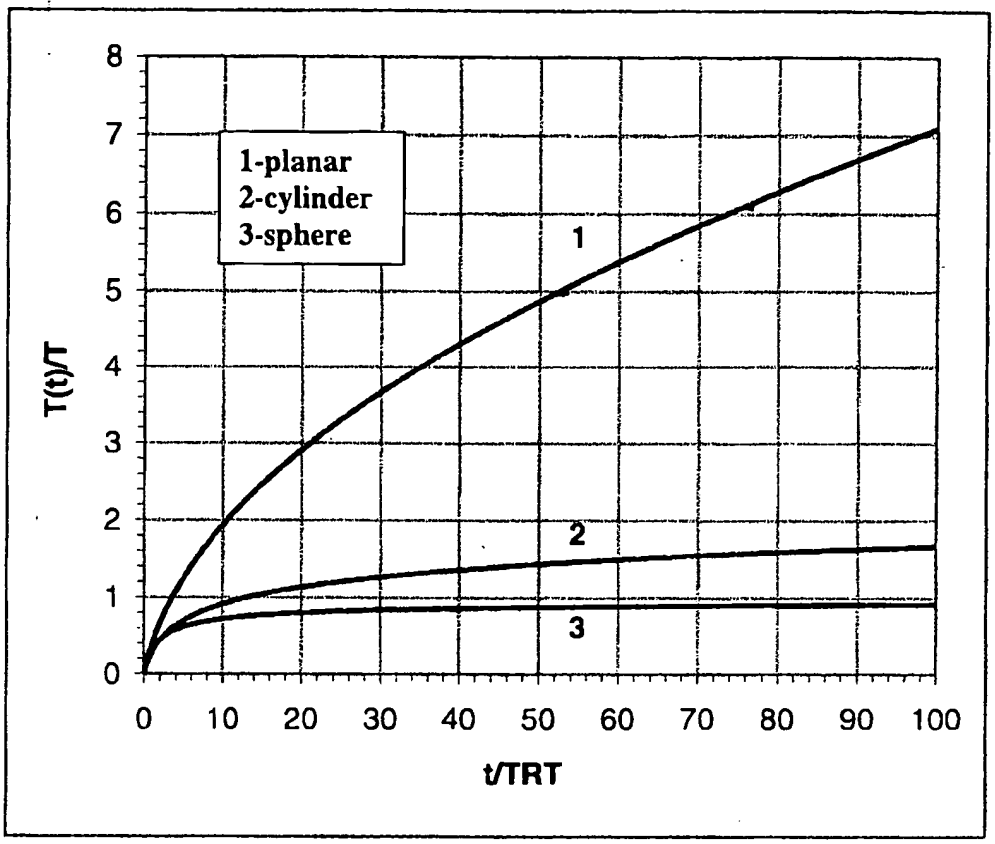
1-planar
2-cylinder
3-sphere
1
2
3
T(t)/T
t/TRT
0
1
2
3
4
5
6
7
8
0
10
20
30
40
50
60
70
80
90
100

Figure 7.

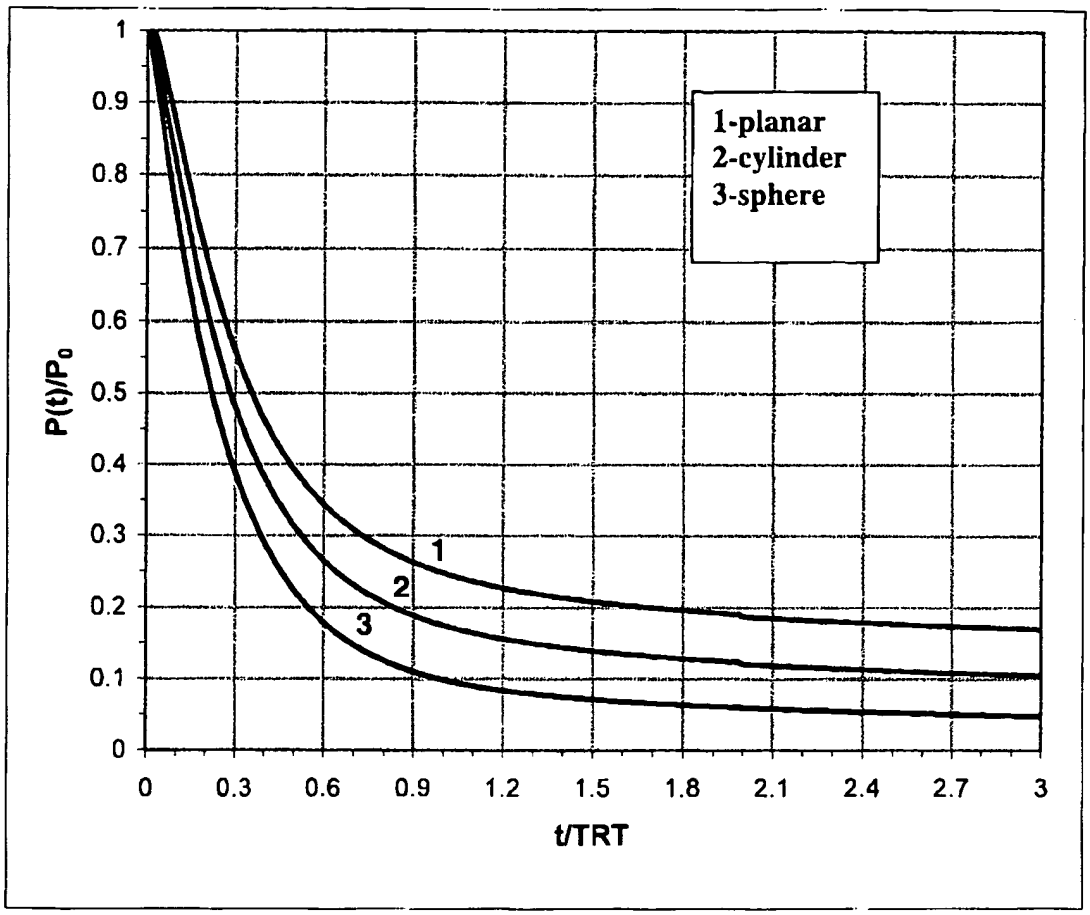
1-planar
2-cylinder
3-sphere
P(t)/P0
t/TRT
1
2
3
0
0.1
0.2
0.3
0.4
0.5
0.6
0.7
0.8
0.9
1
0
0.3
0.6
0.9
1.2
1.5
1.8
2.1
2.4
2.7
3

Figure 8

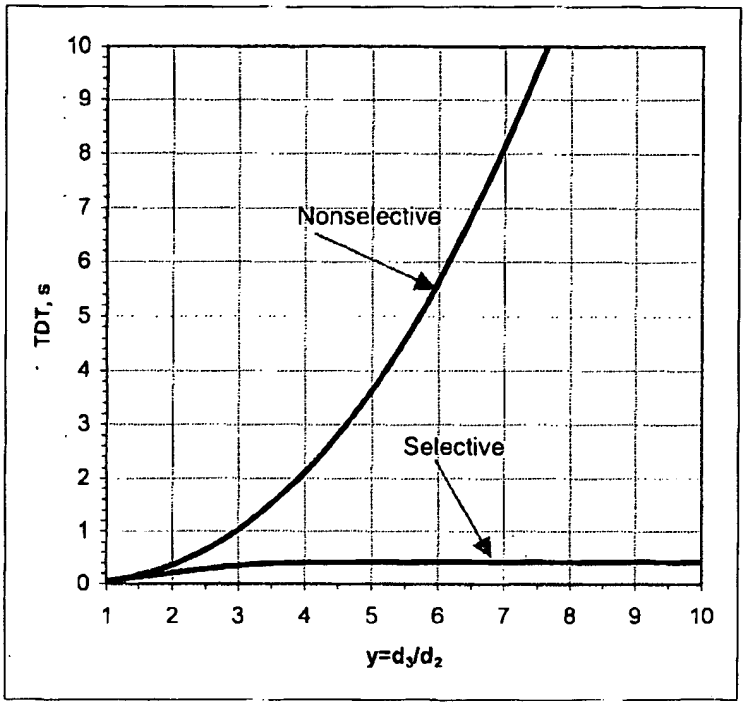
10
9
8
7
6
5
4
3
2
1
0
TDT, s
Nonselective
Selective
1
2
3
4
5
6
7
8
9
10
y=d3/d2

Figure 9a.

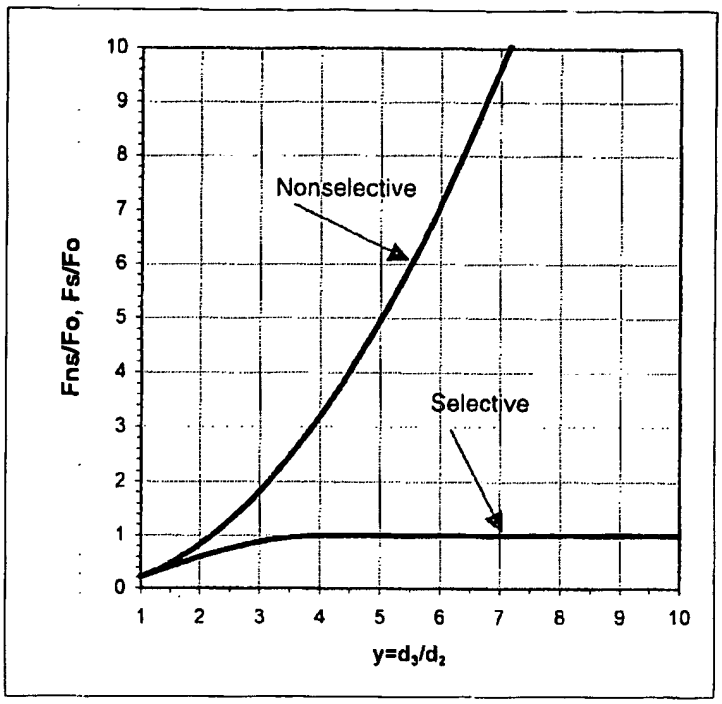

Figure 9b.

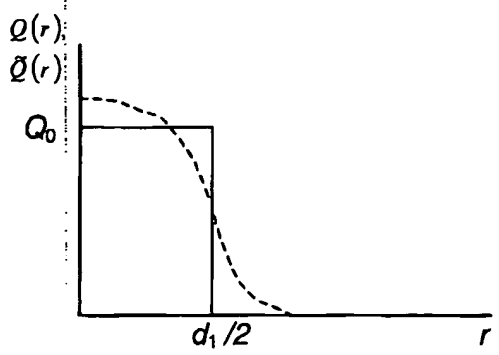

Figure A1.